PROCEEDINGS of the
24th International Congress on Acoustics

October 24 to 28, 2022 in Gyeongju, Korea

ABS-0465

Diffusive surface design using Sierpinski triangle fractal structures

Lingge TAN[1]; Jieun YANG[2]; Jian KANG[3]; Hongpeng XU[1*]

[1] School of Architecture, Harbin Institute of Technology; Key Laboratory of Cold Region Urban and Rural Human Settlement Environment Science and Technology, Ministry of Industry and Information Technology, China

[2] Department of the Built Environment, Eindhoven University of Technology, The Netherlands

[3] Institute for Environmental Design and Engineering, The Bartlett, University College London, UK

ABSTRACT

Diffusive surfaces can be optimally designed for both acoustic and aesthetic purposes. Adapting to the parametric demands of interface design, fractals are widely applied as a fusion of mathematical calculation and artistic design. The Sierpinski triangle is a self-similar structure with a more impressive appearance than conventional acoustic diffusers. However, the acoustic performance of Sierpinski fractal patterns has not been considered. This paper proposes a design of an acoustic diffuser based on the construction rules of the Sierpinski triangle to broaden the effective frequency range. The diffuser is made of triangular blocks of different sizes attached to a plane surface. A series of case studies are examined through numerical simulations based on the boundary element method (BEM) to investigate the effects of the number of iterations, the randomness of block arrangements, and the inclination of block tops. The diffusion performance of a conventional quadratic residue diffuser (QRD) is compared to confirm the advantage of the designed diffuser for broadening the effective frequency range. Furthermore, a workflow of the design and evaluation processes is presented to fabricate samples that could be used to tune the design parameters according to their in-field application demands.

Keywords: Acoustic Diffuser, Sierpinski Triangle, Fractal

1. INTRODUCTION

Diffusive surfaces are critical elements in controlling first-order sound reflections in acoustic spaces (1). They can be used in diverse settings, such as classrooms, meeting rooms, or outdoors, to improve speech clarity, avoid sound focusing (2) and reduce noise levels (3). Diffusers can be designed in many forms, such as hemispheres and cubes (4, 5), one- and two-dimensional grooves (6), curved surfaces (7), or any other topologies (8). The visual perception of a space where acoustic diffusers are installed is strongly determined by the design of the diffuse surfaces, thus acoustic diffusers should be designed by considering both acoustical and aesthetical aspects (9). The combination of these two aspects has only been employed in a few studies (10-12).

Diffusive surfaces have been continuously enriched since the introduction of fractals. The design focus remains mainly on optimizing acoustic performance while also considering the aesthetic needs of users. Xu et al. (13) investigated Sierpinski triangular fractal structures via eye tracking and semantic differences. Compared to traditional QRD diffusers, they found that the proposed diffusers were more attractive. Additionally, the topological surface avoids periodic contours, satisfying both

[1]First author: l.tantan@outlook.com (L. TAN);

Corresponding author:xuhongpeng@hit.edu.cn (H. XU)

aesthetic and acoustic requirements.

The parameter design thinking (PDT) results are appropriate and necessary to deal with the complexity of diffusive surfaces (14). Rather than generating many design variants, PDT focuses on creating detailed, differentiated, rule-based designs. The development of personalized diffusion surfaces based on PDT requires a flexible design method. Shtrepi et al. (8) integrated parametric models with acoustic simulations to provide acoustic visualization feedback for architects during the preliminary design phase. Reinhardt et al. (15) investigated computational design and robotic fabrication methods to develop effective patterns for sound scattering. Peters and Olesen (10) built scattering surfaces with hexagonal elements varying in depth and width with rapid prototyping. Moreover, the use of robots for evaluating diffusive surface designs has been suggested in creative explorations. It allows them to directly tune acoustic and architectural parameters based on the measured results during fabrication.

To propose a diffusive surface that considers both acoustic and aesthetic values, this study develops a methodology for designing modular diffusers based on the Sierpinski-triangle construction rule shown in the authors' previous study (16) and determines the optimized threshold combining the PDT. Four aspects will be investigated:1) Propose a design of a modular diffuser based on the construction rules of the Sierpinski fractals to broaden the effective frequency range; 2) Compare the diffusion performance of a two-dimensional QRD to confirm the advantage in the wide frequency range design; 3) Investigate the effect of the number of iterations, the randomness of arrangement, and the inclination of the tops based on BEM simulations; 4) Develop a workflow for designing rules and evaluating test samples according to the application demands.

2. DESIGN OF DIFFUSIVE SURFACE BASED ON SIERPINSKI TRIANGLE

2.1 Principle

The Sierpinski triangle can be subdivided into smaller triangles (17). We use isosceles right triangles as the fractal pattern base to construct diffusion units that can be incorporated into architectural surfaces (such as walls or facades). Figure 1(a) illustrates the construction of the Sierpinski triangle. It starts from an isosceles right triangle (iteration 0). Then four smaller right-angled triangles are created by connecting the triangle's midpoints, and the center triangle is removed (iteration 1). As a result of repeating the last procedure with the remaining three triangles, nine smaller triangles are created (iteration 2). Using this step, 27 triangles are formed (iteration 3). The combination of two identical Sierpinski triangles forms a rectangle, as shown in Figure 1(b).

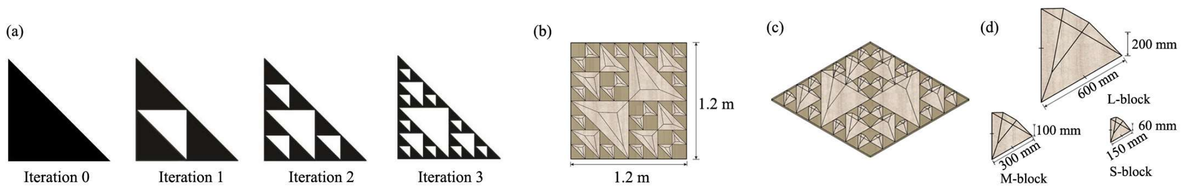

Figure 1 – (a)Construction steps of the Sierpinski triangle pattern; (b) top view and (c) isometric view of the final Sierpinski-triangle diffuser.(d)Dimensions of multi-level modules used.

2.2 Design process

This work proposes Sierpinski-triangle diffusers composed of modules of various sizes attached with a flat plane. Figures 1(b) and 2(c) show the top and isometric views of the final proposed design. The top of pyramid modules is cut by a randomly inclined plane. The diffusers are 1.2 m in length and width, the same size as the basic wall module in Chinese constructions (1.2 m), allowing for easy assembly and rearranging according to audio requirements. Figure 1(d) shows the block dimensions. The dimension of diffusive surface is 1.2 m ×1.2 m ×120 mm.

Diffuser performance is affected by several parameters. Simulations will be used to investigate the influence of these parameters. The scattering surfaces for the case study are shown in Table 1. First, the iteration number is examined in the first group. The authors' previous study (16) showed that diffusers with the fractal iteration patterns combined with different structural heights of triangular blocks (60 mm, 90 mm, and 120 mm) have good diffusion capacity. Similarly, the module pattern is iterated by 1, 2, 3, and 4, while module height varies from 30 mm to 120 mm with a 30 mm interval for different sizes of the blocks. In the second group, a degree of randomness is introduced to break the monotonous pattern. P-values (randomness) of 0.25, 0.50, and 0.75 further quantify the concentration degree of the triangle modules, representing semi-disperse, semi-centralized, and centralized arrangement of modules, respectively. The number of triangular blocks used in A3 and $A3_{(IV)}$ is equivalent. In addition, the sides of the triangular blocks are titled to form triangular pyramids $A3_{(v)}$. Since the facets are angled in pyramidal modules, incident sound waves will be reflected in multiple directions and promote higher diffusion (18). $A3_{(d)}$ is optimized by increasing the height of pyramid module L from 120 mm to 300 mm and enlarging M and S by 2.5 times. Type $A3_{(t)}$ is generated by arbitrarily inclined planes truncating the tops of deep triangular pyramids for improved acoustic performance. The Figure 2 shows the workflow followed in the design and evaluation process. It also outlines the fabrication stage that can be implemented in the future.

Table 1 – Configurations of scattering surfaces considered for case studies.

<table>
<tr><td>Module</td><td colspan="3">Triangular Prism/ Pyramid</td><td colspan="3">Deep Triangular Pyramid</td></tr>
<tr><td>Type</td><td>L</td><td>M</td><td>S</td><td>L</td><td>M</td><td>S</td></tr>
<tr><td>Size(W*H/mm)</td><td>600*120</td><td>300*90</td><td>150*60</td><td>600*300</td><td>300*225</td><td>150*150</td></tr>
<tr><td colspan="7">Groups of Test Samples Affected by Iterations</td></tr>
<tr><td>Type
Iteration</td><td colspan="2">A1
Once</td><td colspan="2">A2
Twice</td><td>A3
Three Times</td><td>A4
Four Times</td></tr>
<tr><td>Top View</td><td colspan="2">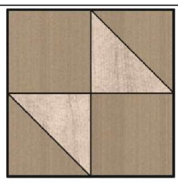</td><td colspan="2">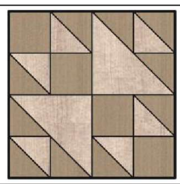</td><td>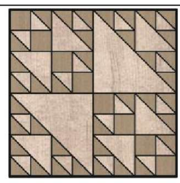</td><td>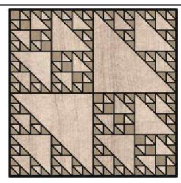</td></tr>
<tr><td>Front View</td><td colspan="2"></td><td colspan="2"></td><td></td><td></td></tr>
<tr><td colspan="7">Groups of Test Samples Affected by Arrangement *</td></tr>
<tr><td>Type
Randomness</td><td colspan="2">A3
P=0.00</td><td colspan="2">$A3_{(II)}$
P=0.25</td><td>$A3_{(III)}$
P=0.50</td><td>$A3_{(IV)}$
P=0.75</td></tr>
<tr><td>Top View</td><td colspan="2">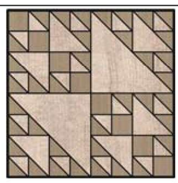</td><td colspan="2">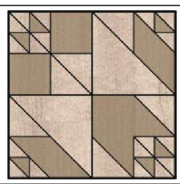</td><td>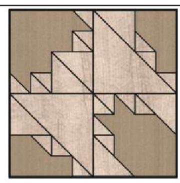</td><td>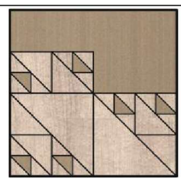</td></tr>
<tr><td>Front View</td><td colspan="2"></td><td colspan="2"></td><td></td><td></td></tr>
<tr><td colspan="7">Groups of Test Samples Affected by Inclination of Tops</td></tr>
<tr><td>Type
Vertical Shape</td><td colspan="2">A3
Prism</td><td colspan="2">$A3_{(V)}$
Pyramid</td><td>$A3_{(d)}$
Deep Pyramid</td><td>$A3_{(t)}$
Truncated Pyramid</td></tr>
<tr><td>Top View</td><td colspan="2">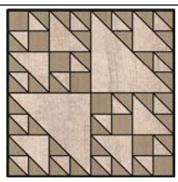</td><td colspan="2">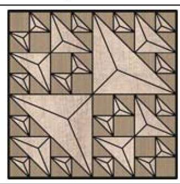</td><td>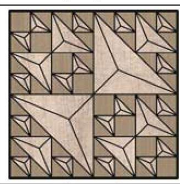</td><td>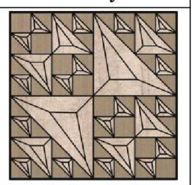</td></tr>
<tr><td>Front View</td><td colspan="2"></td><td colspan="2"></td><td></td><td></td></tr>
</table>

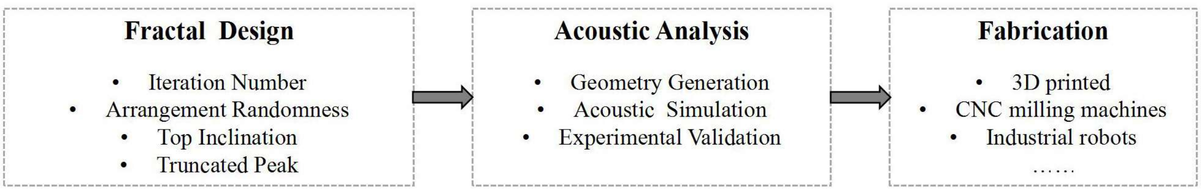

Figure 2 – Workflow:fractal design,acoustic analysis and fabrication

3. METHOD OF EVALUATION OF THE DIFFUSIVE SURFACES

3-D numerical simulations are conducted by using COMSOL Multiphysics 5.4®, BEM in Acoustic Module (19). Scattering surfaces are surrounded by air of which density and speed of sound are given as ρ_0= 1.21 kg/m3 and c_0 = 343 m/s, respectively. All boundaries of scattering structures are assumed to be rigid. We evaluate diffusion performance in a far-field condition following ISO 17497-2 (20). The sound source is located 10 m above the bottom surface of the diffuser, and the receiver arc is placed 5 m above the scattering surface, as shown in Figure 3. There are 35 receiver points on the receiver arc, spaced with 5° intervals. A maximum element size is set to be less than 1/10 of the minimum wavelength of the frequency range of interest. From 100 Hz to 5 kHz, four frequencies per 1/3 octave bands are used for the numerical calculations.

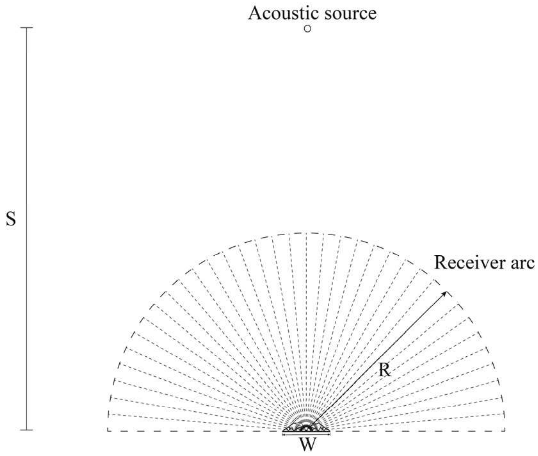

Figure 3 – Numerical simulation setup (S = 10 m, R = 5 m, W = 1.2 m)

According to ISO17497-2, acoustic diffusion coefficients are calculated to determine the performance of diffusers. When the source position is fixed, the diffusion coefficient d_ψ is calculated as follows:

$$d_{\Psi} = \frac{\left(\sum_{i=1}^{n} 10^{L_i/10}\right)^2 - \sum_{i=1}^{n}\left(10^{L_i/10}\right)^2}{(n-1)\sum_{i=1}^{n}\left(10^{L_i/10}\right)^2} \tag{1}$$

where L_i is the sound pressure level (SPL) at the *i-th* receiver position, while n is the number of receivers,and ψ denotes incidence angle. To compare the difference in performance between the samples, only normal incidences were considered, i.e., ψ = 0. After that, a normalized directional diffusion coefficient is calculated for the sample by

$$d_{\psi,n} = \frac{d_\psi - d_{\psi,r}}{1 - d_{\psi,r}} \tag{2}$$

where the directional diffusion coefficients d_ψ and $d_{\psi,n}$ represent the sample and reference plane surfaces, respectively. Following the calculation of the normalized diffusion coefficients, the coefficients are averaged in bands of 1/3 octave.

4. RESULTS

Figure4 shows the normalized diffusion coefficients $d_{0,n}$ of the diffusers affected by iterations with various heights in the first group. From 315 Hz, all scattering surfaces in group 1 present similar or worse diffusion properties than plane surfaces below 315 Hz, implying that their diffusion performances are similar or worse than a plane surface. In the frequency range of 315 Hz to 5 kHz, A1, A2, and A4 tend to perform worse in higher frequencies, especially above 2 kHz, while A3 performs better in these bands. In addition, the diffusion coefficients for A1, A2, and A3 increase as the number of iterations increases. However, A4 has lower diffusion coefficients than A3, showing an optimum number of iterations to design diffusers that perform well. Consequently, as the number of iterations increases, the triangular blocks on the base panels are covered by 25%, 44%, 57%, and 68%, respectively. When the coverage area increases from 25% to 57%, the normalized diffusion coefficients vary from 0.46 to 0.61 at 1 kHz, then decrease in higher frequencies due to the absence of surface irregularities. Furthermore, in diffuser configurations, many wells are formed between triangular blocks (colored white), whose size decreases as the number of iterations increases. When the wavelengths are in the mid-to-high frequency range, the wells become comparable in size. As a result, waves would be scattered specularly due to locally reacting wells.

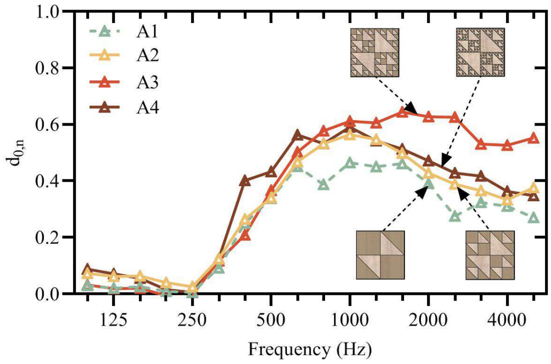

Figure 4 –Normalized diffusion coefficients of the diffusers in group A

Figure 5 shows the normalized diffusion coefficients $d_{0,n}$ of the diffusers affected by arrangement in the second group. By altering the scattering surface topology, group 2 intends to verify the diffusion capacity of the diffuser designed using fractal sequences over other structures. A decline in diffusion coefficients is observed when triangular modules become more random. Among the four diffusion coefficients, A3 has the highest value (P = 0), followed by $A3_{(II)}$ (P = 0.25), $A3_{(III)}$ (P = 0.50), and $A3_{(IV)}$ (P = 0.75) sequentially. $A3_{(II)}$ decreases normalized diffusion coefficients over 800 Hz compared to A3. Comparisons of $A3_{(II)}$ and $A3_{(III)}$ show $A3_{(II)}$have superior diffusion performance. Furthermore, $A3_{(IV)}$ show almost similar diffusion performance to $A3_{(III)}$, although slightly worse above 2 kHz than $A3_{(III)}$. The reason is that the dispersion for the triangular blocks varies in degree, resulting in varying well sizes and widths. Then specular reflections form on some surfaces, affecting scattering uniformity.

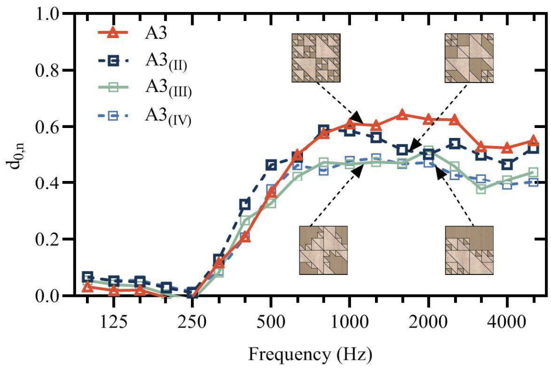

Figure 5 –Normalized diffusion coefficients of the diffusers in group B

The threshold for diffuser design is the third group compared and optimized type A3 as three iterations of the modules. Figure 6 shows the normalized diffusion coefficients $d_{0,n}$ of diffusers influenced by top inclination. From 250 Hz to 1 kHz, type $A3_{(v)}$ with pyramid modules shows better diffusion capacity than type A3 with prism modules, while below 2.5 kHz, they are comparable, and then $A3_{(v)}$ has higher diffusion coefficients than A3 in the range of 3.15 - 5 kHz. The diffusion coefficients of $A3_{(v)}$ increase as frequencies increased in the frequency range of interest. When $A3_{(d)}$ and $A3_{(v)}$ are compared, $A3_{(d)}$ presents comparable or better diffusion performance from 250 Hz to 1 kHz. At the same time, a notable peak is observed around 1kHz for $A3_{(d)}$, suggesting that the use of higher prismatic modules can enhance the diffusion capability of the diffuser at mid-low frequencies.

Diffusion coefficients of $A3_{(d)}$, however, decrease in mid-high frequency range. A further effect of the angle between the two sets of modules is the generation of specular reflections (18). In addition, type $A3_{(t)}$ with truncated pyramid modules presents broadband diffusion performance, which is suitable for further optimization. Compared to $A3_{(v)}$, $A3_{(t)}$ shows better performance between 250 Hz and 500 Hz, with a small peak around 500 Hz band. At frequencies above 500 Hz, $A3_{(v)}$ displays a similar capacity as $A3_{(v)}$. Compared to A3, the coefficients of $A3_{(t)}$ are higher in the mid-low frequency range of 250 to 800 Hz and the mid-high frequency range of 3.15 to 5 kHz. Figure 6 also compares the diffusion coefficients of QRD with two-dimensional gratings (N=7). $A3_{(t)}$ presents more advantages of broadband diffusion than QRD in the 250Hz - 5 kHz frequency band.

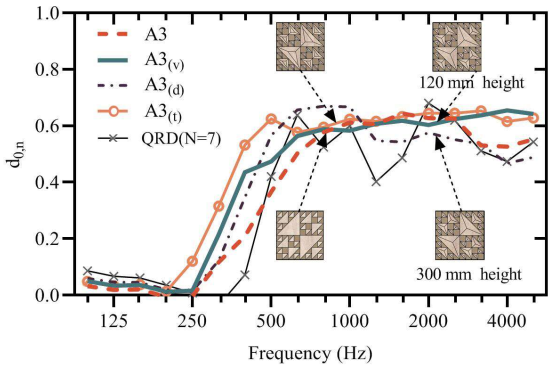

Figure 6 –Normalized diffusion coefficients of the diffusers in group C.Normalized diffusion coefficients of QRD with 2-dimensional gratings (N = 7, black line) are also compared.

5. CONCLUSIONS

This study showed that fractal acoustic diffusers presented superior bandwidth and low-frequency capacity than conventional QRDs. The proposed diffusers were designed based on the Sierpinski-triangle fractal, composed of triangles of different sizes. Sierpinski-triangle diffusers were constructed from triangular modules with varying cross sections and heights. Further, the performance-optimizing design for the tilted tops of the triangular modules was discussed. Using 3D numerical simulations based on a BEM, we investigated the effects of fractal iterations, randomness degree of module arrangements, and inclination of module tops on normal-incidence diffusion coefficients. The following conclusions can be made by the results:

(1) Fractal acoustic diffusers combined with triangular modules of varying heights demonstrated high diffusion capability in the frequency range between 250 Hz and 5 kHz. A high-diffusion performance was achieved by applying an optimum number of iterations (three in this study).

(2) Fractal diffusers performed better in the module arrangement with a lower randomness degree when the scattering surface topology was changed.

(3) Diffusion performances of fractal diffusers are significantly enhanced when the module shape was changed from prism to pyramid in the high-frequency range (2 - 5 kHz). Increasing the height of the pyramid module and reducing the angle between the modules improved the diffusion capacity of the diffuser at mid-low frequencies (＜1 kHz) but deteriorated it at high and mid frequencies (>1 kHz).

(4) Diffusers composed of truncated pyramid modules demonstrated enhanced diffusion performance in a broad range of frequency. In comparison to conventional diffusers of the same size, the fractal patterns with various sizes of truncated pyramid modules produced a better diffusion performance, especially in the mid-low frequency range.

Furthermore, we present a workflow of the design and evaluation processes to fabricate samples that can be used to refine design parameters according to the needs of the field application. In the present study, Sierpinski-triangle diffusers were compared under normal-incidence conditions to compare performance differences due to design parameters. The performance of diffusion under oblique- and random-incidence conditions would be beneficial to study in future research. In addition, Sierpinski-triangle diffusers can also be investigated in a real-sized room to enhance the room's acoustics and determine the most effective combination pattern.

ACKNOWLEDGEMENTS

This research was funded by the China Scholarship Council (No.201906120322), the National Natural Science Foundation of China (No.51778169), and the Ministry of Science and Technology of China (No.G2021179030L).

REFERENCES

1. Haan C, Fricke FR. An evaluation of the importance of surface diffusivity in concert halls. Applied Acoustics. 1997;51(1):53-69.
2. Cox TJ, D'Antonio P. Acoustic Absorbers and Diffusers: Theory, Design and Application (3rd ed.): CRC Press; 2016.
3. Yang H-S, Kang J, Cheal C. Random-Incidence Absorption and Scattering Coefficients of Vegetation. Acta Acustica united with Acustica. 2013;99:379-88.
4. Yong Jeon J, Chan Lee S, Vorländer M. Development of scattering surfaces for concert halls. Applied Acoustics. 2004;65(4):341-55.
5. Kang J. Experimental Approach to the Effect of Diffusers on the Sound Attenuation in Long Enclosures. 1995;2(1):391-402.
6. Kim YH, Jang HS, Jeon JY. Characterizing diffusive surfaces using scattering and diffusion coefficients. Applied Acoustics. 2011;72(11):899-905.
7. Cox TJ. Designing curved diffusers for performance spaces. Journal of the Audio Engineering Society. 1996;44(5):354-64.
8. Shtrepi L, Mendéz Echenagucia T, Badino E, Astolfi A. A performance-based optimization approach for diffusive surface topology design. Building Acoustics. 2020;28(3):231-47.
9. Cox TJ, editor Proceedings of the Institute of Acoustics ACOUSTIC DIFFUSERS : THE GOOD , THE BAD AND THE UGLY2006.
10. Peters B. Integrating Sound Scattering Measurements in the Design of Complex Architectural Surfaces:Informing a parametric design strategy with acoustic measurements from rapid prototype scale models. Denmark, Europe2010.
11. Jensen M. Robotic Fabrication of Acoustic Geometries: an explorative and creative design process within an educational context. 2019;6:34-45.
12. Shtrepi L, Menichelli J, Astolfi A, Mendez Echenagucia T, Masoero MC. Improving scattering surface design with rapid feedback by integrating parametric models and acoustic simulation. The Journal of the Acoustical Society of America. 2017;142(4):2499-.
13. Xu HP, Ni FW, Wu JM, editors. Multi-level modular wooden diffusers based on fractal theory. 2018 World Conference on Timber Engineering, WCTE 2018, August 20, 2018 - August 23, 2018; 2018; Seoul, Korea, Republic of: World Conference on Timber Engineering (WCTE).
14. Oxman R. Thinking difference: Theories and models of parametric design thinking. Design Studies. 2017;52:4-39.
15. Reinhardt D, Cabrera D, Jung A, Watt R. Towards a Micro Design of Acoustic Surfaces : Robotic Fabrication of Complex Pattern Geometries. Cham: Springer International Publishing; 2016. 136-49 p.
16. Tan L, Yang J, Kang J, Xu H. Sound-scattering properties of Sierpinski triangle fractal structures in the near field. Applied Acoustics. 2022;196:108892.
17. Rasouli Kenari A, Solaimani M. Optical properties of two dimensional fractal shaped nanostructures: Comparison of Sierpinski triangles and Sierpinski carpets. Optics Communications. 2020;474.
18. Cox T. Room acoustics diffusers: pyramids and wedges. International Congress on Sound and Vibration (ICSV24); London2017.
19. COMSOL. COMSOL Multiphysics® v. 5.4. COMSOL AB, Stockholm, Sweden.
20. BS ISO 17497-2:2012 Acoustics. Sound-scattering properties of surfaces. Measurement of the directional diffusion coefficient in a free field: BSI Standards Limited; 2012.